Contribution from the Department of Chemistry,
Washington State University, Pullman, Washington 99164-4630

Magnetic and Structural Correlations in $[(C_5H_5N)NH_2]_2Cu_2Cl_6$ and $[(C_5H_5N)NH_2]_2Cu_2Br_6 \cdot H_2O$

Joan T. Blanchette and Roger D. Willett*

Received October 23, 1987

The crystal structures of the title compounds, (3-aminopyridinium)$_2Cu_2Cl_6$ and (3-aminopyridinium)$_2Cu_2Br_6 \cdot H_2O$, have been determined. The chloride dimer is monoclinic [a = 7.623 (1) Å, b = 14.700 (2) Å, c = 8.121 (1) Å, β = 93.09 (1)°] and crystallizes in the space group $P2_1/a$, while the bromide dimer is monoclinic [a = 19.096 (5) Å, b = 6.729 (1) Å, c = 19.499 (5) Å, β = 126.89 (1)°] and crystallizes in the space group $C2/c$. The two compounds contain similar species, with each copper ion having a distorted-trigonal-bipyramidal geometry involving four halide ions and the amino nitrogen from the pyridinium ion. Pairs of copper(II) ions are joined by two Cu–X–Cu (X = Cl^-, Br^-) bridges to form the centrosymmetric dimer structures. The chloride dimer is symmetrically bibridged, while the bromide dimer is of the asymmetrically bibridged type. The latter contains a water of hydration, the structural effects of which are important magnetically. The copper ions in the chloride dimer show principally an angular distortion from trigonal-bipyramidal geometry, and the Cu–Cl–Cu bridging angle in the dimer is 94.9 (1)°. In the bromide compound, the coordination is distorted more toward a 4 + 1 coordination geometry around each copper atom, with a Cu–Br–Cu bridging angle of 93.4 (1)° and an interdimer Br···Br distance of 3.728 Å. The magnetic susceptibilities of the two compounds were measured between 2.0 and 280 K. The results have been interpreted in terms of ferromagnetic coupling within the chloride dimer ($J_{Cl}/k \cong 30$ K). A substantial antiferromagnetic coupling is observed for the bromide salt, and it is concluded that the magnetic dimer consists of copper ions from two adjacent structural dimers. The structural chemistry of five-coordinate copper(II) chloride species is summarized, and it is concluded that the folded 4 + 1 coordination geometry is the favored geometry.

Introduction

The study of the magnetostructural correlations is of interest not only in inorganic chemistry but also in fields ranging from solid-state physics to bioinorganic chemistry. Among solid-state physicists, the interest in the physics of low-dimensional magnetic systems has brought about a renewed interest in magnetic interactions in solids.[1] Many bioinorganic chemists are interested in the interactions of magnetically coupled metal ions in metalloproteins and metalloenzymes, as the study of these interactions could lead to an explanation of the role of these essential metal ions in the functioning of the protein or enzyme.[2] The work of the inorganic chemist is vital to the physicist's and biochemist's study of magnetic interactions in exchange-coupled systems. By synthesizing and characterizing various new types of magnetic systems, the inorganic chemist can provide models for magnetostructural correlations that can then be applied both to the more specific low-dimensional models of the solid-state physicists[3] and to the often more complex magnetic systems in proteins and enzymes.[4]

In our laboratory, the study of magnetostructural correlations has centered on copper(II) halide compounds.[5] Copper(II) compounds are spin $^1/_2$, so there is only one magnetic orbital per Cu atom, and thus the electronic properties of the single ion are easily described. In compounds, however, the flexible coordination geometry of the copper(II) and the existence of both "coordinated" and "semicoordinated" ligands have resulted in electronic structures that are not well characterized and exist in a wide array of superexchange pathways.[6] This variety in the structure and magnetics of copper(II) compounds makes copper(II) systems as interesting to the inorganic chemist as they are to the physicist and the biochemist. One of the goals in our laboratory, which is also of interest to solid-state physicists, is the design and characterization of a spin $^1/_2$ isotropic (Heisenberg) ferromagnetic linear-chain system.[7] Copper(II) systems are also of interest to the bioinorganic chemist because of the many proteins and enzymes (e.g., hemocyanin, tyrosinase) that contain copper(II) magnetic interactions.[8]

The project described in this paper is a further study of the magnetostructural correlations in copper(II) compounds by means of the synthesis, X-ray crystal structure determination, magnetic susceptibility measurements, and analysis of two new copper(II) halide compounds. As a result of this project, we have discovered an unusual exchange pathway in copper(II) halide dimers.

Materials and Methods

Syntheses. (3AP)$_2Cu_2Cl_6$. A 1.2-g sample of 3-aminopyridine was dissolved in an aqueous solution of 50% ethanol. A 4.0-g sample of $CuCl_2 \cdot 2H_2O$ was added with stirring. The solution was continuously stirred while 1 M HCl was added dropwise until the solution became clear. The solution was evaporated over low heat until crystals began to form. The red, plate-like crystals of (3AP)$_2Cu_2Cl_6$ (3AP ≡ 3-aminopyridinium) were recrystallized by temperature-gradient crystallization.[9]

(3AP)$_2Cu_2Br_6 \cdot H_2O$. A 1.2-g sample of 3-aminopyridine was dissolved in 50% ethanol. To this was added 24 mL of 1 M $CuBr_2$ (aqueous) and 24 mL of absolute ethanol. The solution was stirred continuously as 1 M HBr was added to make the solution clear. The dark violet, essentially opaque platelike crystals were grown and recrystallized as above. For both syntheses, it is necessary to avoid higher acid concentrations so as not to form the dicationic (3AP)CuX_4 salts.

X-ray Crystallography and Structure Solution. X-ray crystal structure data collections were performed on a Nicolet R3m/E diffractometer system.[10] The crystal used for the chloride dimer had dimensions 0.40 × 0.40 × 0.05 mm. The system is monoclinic, $P2_1/a$, with a = 7.623 (2) Å, b = 14.700 (2) Å, c = 8.121 (1) Å, and β = 93.09 (1)° (λ = 0.71069 Å) with ρ_{calcd} = 1.94 g/cm^3 for Z = 2. The structure solution and refinement were accomplished with use of the version 4.1 SHELX programs.[11] A final value of $R = \sum||F_o| - |F_c||/\sum|F_o| = 0.029$ and $R_w = (\sum w(F_o - F_c)^2/\sum w|F_o|^2)^{1/2} = 0.044$ was obtained. For the bromide dimer, the crystal used had dimensions 0.08 × 0.22 × 0.36 mm. This

(1) Willett, R. D., Gatteschi, D., Kahn, O. Eds. *Magneto-Structural Correlation in Exchange Coupled Systems*; NATO ASI Series C140; D. Reidel: Dordrecht, The Netherlands, 1985.
(2) Solomon, E. I.; Wilcox, D. E. in ref 1; p 463.
(3) Bonner, J. C. *J. Appl. Phys.* **1978**, *49*, 1299. De Jongh, L. J.; Miedena, A. R. *Adv. Phys.* **1974**, *23*, 1. Steiner, M.; Villain, J.; Windsor, C. G. *Adv. Phys.* **1976**, *25*, 87.
(4) Vallee, B. L.; Williams, R. J. P. *Proc. Natl. Acad. Sci. U.S.A.* **1968**, *59*, 498.
(5) Willett, R. D.; Grigereit, T.; Halvorson, K.; Scott, B. *Proc.—Indian Acad. Sci., Chem. Sci.* **1987**, *98*, 147.
(6) Willett, R. D.; Geiser, U. *Croat. Chem. Acta* **1984**, *57*, 737.
(7) Groenendijk, H. A.; Blote, H. W. J.; Van Duyneveldt, A. J.; Gaura, R. M.; Landee, C. P.; Willett, R. D. *Physica B+C (Amsterdam)* **1981** *106B+C*, 45. Hoogerbeets, R.; Weigers, S. A. J.; Van Dugneveldt, A. J.; Willett, R. D.; Geiser, U. *Physica B+C (Amsterdam)* **1984**, *125B+C*, 135.
(8) (a) Solomon, E. I. In *Copper Proteins*, Spiro, T. G., Ed.; Wiley-Interscience: New York, 1986; Chapter 2. (b) Dooley, D. M.; Scott, R. A.; Ellinghaus, E.; Solomon, E. I.; Gray, H. B. *Proc. Natl. Acad. Sci. U.S.A.* **1978**, *75*, 3019.
(9) Arend, H.; Huber, W.; Mischgofsky, F. H.; Richter-Van Leeuwen, G. K. *J. Cryst. Growth* **1978**, *43*, 213.
(10) Campana, C. F.; Shepherd, D. F.; Litchman, W. M. *Inorg. Chem.* **1981**, *20*, 4039.
(11) Sheldrick, G. *SHELXTL*, Version 4.1; Nicolet Analytical Instruments: Madison, WI, 1984.

0020-1669/88/1327-0843$01.50/0 © 1988 American Chemical Society

Table I. X-ray Data Collection Parameters

	bis(3-aminopyridinium) hexachlorodicuprate(II)	bis(3-aminopyridinium) hexabromodicuprate(II) hydrate
empirical formula	$C_{10}H_{14}Cl_6Cu_2N_4$	$C_{10}H_{16}Br_6Cu_2N_4O$
mol wt	530.06	814.78
diffractometer syst	Nicolet R3m/E	Nicolet R3m/E
cryst class:	monoclinic	monoclinic
space group:	$P2_1/a$	$C2/c$
lattice consts		
a, Å	7.623 (1)	19.096 (5)
b, Å	14.700 (2)	6.729 (1)
c, Å	8.121 (1)	19.499 (5)
β, deg	93.09 (1)	126.89 (1)
V, Å^3	908.6 (2)	2002 (2)
	based on 25 reflcns in the range $35° < 2\theta < 40°$	based on 25 reflcns in the range $26° < 2\theta < 27°$
$F(000)$	1047.8	1519.6
radiation	Mo Kα with graphite monochromator	Mo Kα with graphite monochromator
cryst size, mm^3	0.40 × 0.40 × 0.05	0.08 × 0.22 × 0.36
abs coeff, cm^{-1}	32.38	140.9
ρ_{calcd}, g/cm^3	$\rho = 1.94$ ($Z = 2$)	$\rho = 2.71$ ($Z = 4$)
type of abs cor	numerical	numerical
max transmissn	0.607	0.319
min transmissn	0.184	0.052
temp, °C	20	20
data collcn technique	ω scan	ω scan
scan range	0.85	0.9
scan speed, deg/min	3.00 (min); 29.30 (max)	4.00 (min); 29.30 (max)
check reflcns[a]	1,1,0; 2,4,–1	3,1,–4; 7,1,–5; 2,2,5
tot. no. of reflcs	3687	2038
2θ(max), deg	50	50
no. of unique reflcns	3601 with 3028 with $F > 3\sigma(F)$	1978 with 1448 with $F > 3\sigma(F)$
R for equiv reflcns		0.0229
hkl	$-11 < h < 11$	$0 < h < 23$
	$0 < k < 22$	$0 < k < 8$
	$0 < l < 12$	$-24 < l < 24$
struct soln package	Nicolet SHELXTL	Nicolet SHELXTL
struct soln technique	direct methods	direct methods
R[b]	0.029	0.055
R_w	0.044	0.066
g	0.00054	0.0026
function minimized	$\sum w(\|F_o\| - \|F_c\|)^2$	$\sum w(\|F_o\| - \|F_c\|)^2$
goodness of fit	1.422	1.042
$\|\Delta/\sigma\|$(mean)	0.010	0.002
$\|\Delta/\sigma\|$(max)	0.043	0.018
tot. no. params refined	101	106
thermal params	anisotropic on all non-H atoms	anisotropic on all non-H atoms
hydrogen atoms	constrained to C–H and N–H = 0.96 Å; thermal params fixed at 20% above heavy-atom values	constrained to C–H and N–H = 0.96 Å; thermal params fixed at 20% larger than heavy-atom values
largest peak on final diff map, e/Å^3	0.9 near Cl (2)	1.6 near Cu
most negative peak on final diff map, e/Å^3	–0.6	–1.3
extincn cor	yes	no

[a] Monitored every 100 reflections. [b] $R = \sum||F_o| - |F_c||/|F_o|)^2$. [c] $R_w = [\sum w(|F_o| - |F_c|)^2/\sum w|F_o|^2]^{1/2}$; $w = 1/[\sigma^2(F) + g(F)^2]$.

Table II. Atomic Coordinates (×10^4) and Isotropic Thermal Parameters (Å^2 × 10^3) for $(3AP)_2Cu_2Cl_6$[a]

	x	y	z	U
Cu	1496 (1)	838 (1)	4650 (1)	24 (1)
Cl (1)	943 (1)	2278 (1)	3723 (1)	28 (1)
Cl (2)	–1025 (1)	245 (1)	3326 (1)	47 (1)
Cl (3)	3635 (1)	273 (1)	2665 (1)	31 (1)
N (1)	3690 (2)	1297 (1)	5965 (2)	23 (1)
N (2)	3257 (2)	1904 (1)	10279 (2)	33 (1)
C (1)	3503 (2)	1828 (1)	7411 (2)	22 (1)
C (2)	3390 (2)	2774 (1)	7340 (2)	28 (1)
C (3)	3225 (3)	3263 (1)	8797 (2)	34 (1)
C (4)	3157 (3)	2817 (1)	10274 (2)	35 (1)
C (5)	3434 (2)	1403 (1)	8921 (2)	28 (1)

[a] The equivalent isotropic U is defined as one-third of the trace of the orthogonalized U_{ij} tensor.

Table III. Bonding Parameters for $(3AP)_2Cu_2Cl_6$

	(a) Bond Lengths (Å)		
Cu–Cl (1)	2.279 (1)	N(2)–C(4)	1.344 (3)
Cu–Cl (2)	2.320 (1)	N(2)–C(5)	1.339 (2)
Cu–Cl (3)	2.496 (1)	C(1)–C(2)	1.395 (2)
Cu–N(1)	2.049 (1)	C(1)–C(5)	1.380 (2)
Cu–Cl(2A)	2.330 (1)	C(2)–C(3)	1.396 (3)
Cl(2)–Cu(A)	2.330 (1)	C(3)–C(4)	1.371 (3)
N(1)–C(1)	1.423 (2)		
	(b) Bond Angles (deg)		
Cl(1)–Cu–Cl(2)	93.5 (1)	Cu–Cl(2)–Cu(A)	94.9 (1)
Cl(1)–Cu–Cl(3)	102.2 (1)	Cu–N(1)–C(1)	119.2 (1)
Cl(2)–Cu–Cl(3)	92.4 (1)	C(4)–N(2)–C(5)	123.7 (2)
Cl(1)–Cu–N(1)	89.9 (1)	N(1)–C(1)–C(2)	121.4 (1)
Cl(2)–Cu–N(1)	175.7 (1)	N(1)–C(1)–C(5)	119.7 (1)
Cl(3)–Cu–N(1)	84.4 (1)	C(2)–C(1)–C(5)	118.9 (1)
Cl(1)–Cu–Cl(2A)	146.6 (1)	C(1)–C(2)–C(3)	119.1 (2)
Cl(2)–Cu–Cl(2A)	85.1 (1)	C(2)–C(3)–C(4)	120.3 (2)
Cl(3)–Cu–Cl(2A)	111.0 (1)	N(2)–C(4)–C(3)	118.4 (2)
N(1)–Cu–Cl(2A)	90.5 (1)	N(2)–C(5)–C(1)	119.6 (2)

system is monoclinic, $C2/c$, with $a = 19.096$ (5) Å, $b = 6.729$ (1) Å, $c = 19.499$ (5) Å, and $\beta = 126.89$ (1)° ($\lambda = 0.71069$ Å) with $Z = 4$ for $\rho_{calcd} = 2.71$ g/cm^3. Again, the version 4.1 SHELX programs were used for structure solution and refinement. The final values of $R = 0.055$ and $R_w = 0.066$ were obtained. Data collection parameters are given in Table I and final positional and isotropic thermal parameters in Tables II and IV with selected bond lengths and angles given in Tables III and V.

Table IV. Atomic Coordinates ($\times 10^4$) and Isotropic Thermal Parameters ($Å^2 \times 10^3$) for $(3AP)_2Cu_2Br_6 \cdot H_2O$[a]

	x	y	z	U
Cu	912 (1)	1132 (2)	1081 (1)	24 (1)
Br (1)	81 (1)	−1976 (2)	668 (1)	31 (1)
Br(2)	2216 (1)	−646 (2)	1514 (1)	30 (1)
Br(3)	220 (1)	2447 (2)	1689 (1)	34 (1)
N(1)	3426 (5)	4134 (14)	1317 (6)	36 (5)
N(2)	1516 (5)	3867 (11)	1322 (5)	23 (4)
C(2)	2939 (7)	3837 (15)	1593 (6)	32 (5)
C(3)	2069 (6)	4238 (13)	1068 (6)	22 (5)
C(4)	1706 (6)	4962 (14)	250 (6)	27 (5)
C(5)	2227 (7)	5198 (15)	−20 (7)	34 (6)
C(6)	3094 (7)	4773 (16)	532 (7)	36 (6)
U	5000	1857 (12)	2500	44 (7)

[a] The equivalent isotropic U is defined as one-third of the trace of the orthogonalized U_{ij} tensor.

Table V. Bonding Parameters for $(3AP)_2Cu_2Br_6 \cdot H_2O$

	(a) Bond Lengths (Å)		
Cu–Br(1)	2.451 (2)	N(1)–C(6)	1.328 (17)
Cu–Br(2)	2.413 (2)	N(2)–C(3)	1.433 (19)
Cu–Br(3)	2.412 (2)	C(2)–C(3)	1.356 (14)
Cu–N(2)	2.070 (8)	C(3)–C(4)	1.390 (16)
Cu–Br(1A)	2.791 (2)	C(4)–C(5)	1.386 (23)
N(1)–C(2)	1.341 (21)	C(5)–C(6)	1.358 (15)
	(b) Bond Angles (deg)		
Br(1)–Cu–Br(2)	91.2 (1)	Cu–Br(1)–Cu(A)	93.4 (1)
Br(1)–Cu–Br(3)	92.1 (1)	C(2)–N(1)–C(6)	123.0 (10)
Br(2)–Cu–Br(3)	139.9 (1)	Cu–N(2)–C(3)	120.1 (7)
Br(1)–Cu–N(2)	174.7 (2)	N(1)–C(2)–C(3)	119.8 (11)
Br(2)–Cu–N(2)	92.5 (3)	N(2)–C(3)–C(2)	121.8 (10)
Br(3)–Cu–N(2)	87.5 (3)	N(2)–C(3)–C(4)	119.7 (9)
Br(1)–Cu–Br(1A)	86.6 (1)	C(2)–C(3)–C(4)	118.5 (13)
Br(2)–Cu–Br(1A)	109.3 (1)	C(3)–C(4)–C(5)	119.9 (9)
Br(3)–Cu–Br(1A)	110.8 (1)	C(4)–C(5)–C(6)	119.1 (12)
N(2)–Cu–Br(1A)	88.5 (2)	N(1)–C(6)–C(5)	119.6 (15)
	(c) Interdimer Contacts (Å)		
Br(3)···Br(3)	3.728 (2)	Br(2)···Br(3)	4.159 (2)
Br(1)···Br(3)	4.181 (2)	Br(2)···N(2)	3.391 (8)
Br(1)···N(2)	3.573 (8)	Br(2)···H(2B)	2.432 (2)
Br(1)···H(2A)	2.639 (2)		

Anisotropic thermal parameters and $|F_o|$ and $|F_c|$ values are available as supplementary material. Scattering factors are taken from ref 12.

Magnetic Susceptibility and EPR Measurements. Magnetic data collections were made on a PAR vibrating-sample magnetometer over a temperature range of 2.0–280 K. An applied magnetic field of 5000 G for the chloride and 10 120 G for the bromide was used for the temperature range of 2.0–85 K, and a field of 8491 G was applied from 85 to 280 K. A germanium resistance thermometer was used for the low-temperature range, and a thermocouple was used to measure the higher temperatures. The diamagnetic correction term was -284×10^{-6} emu/mol for the chloride and -360×10^{-6} emu/mol for the bromide. The temperature-independent paramagnetism was taken as 120 emu/mol of dimer for both compounds.

Powder electron paramagnetic resonance (EPR) spectra were run on a Varian E3 EPR spectrometer at room temperature and at liquid-nitrogen temperature (77 K) on both the chloride and bromide compounds. For the $(3AP)_2Cu_2Cl_6$ sample, a single broad peak was observed both at room temperature and at 77 K, with a peak width of 960 G and $g = 2.12$ at room temperature and a peak width of 950 G and $g = 2.11$ at 77 K. For $(3AP)_2Cu_2Br_6 \cdot H_2O$, a single peak was again observed at both temperatures, with a peak width of 320 G and $g = 2.10$ at room temperature and a peak width of 235 G and $g = 2.09$ at 77 K.

Results and Discussion

Crystal Structure Description. The structures of these two compounds (Figures 1 and 2) consist of bibridged copper(II) halide dimers with amino-coordinated 3-aminopyridinium cations. The chloride salt is a symmetrically bibridged dimer with a bridging angle of 94.9 (1)°, and nearly trigonal-bipyramidal coordination

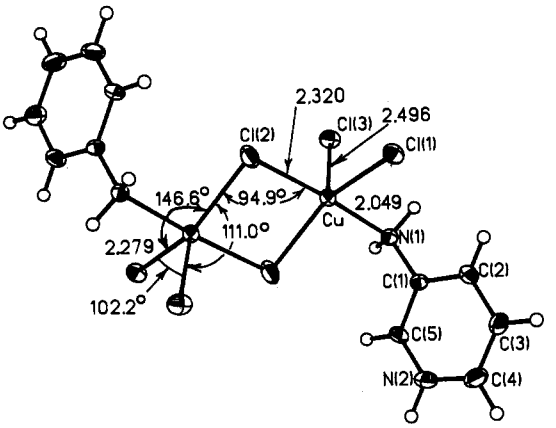

Figure 1. Illustration of the dimer in $(3AP)_2Cu_2Cl_6$.

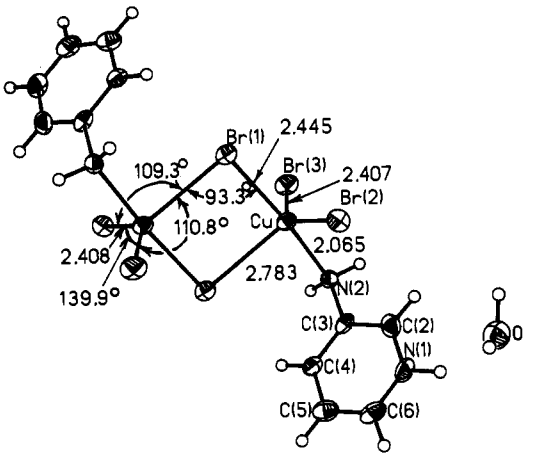

Figure 2. Illustration of the dimer in $(3AP)_2Cu_2Br_6 \cdot H_2O$.

geometry around each copper(II) atom. The bromide dimer is of the asymmetrically bribridged type, with a bridging angle of 93.4°, and a significant 4 + 1 distortion of the coordination geometry can be seen, as evidenced by the one longer Cu–Br bond. The bromide dimer also contains one water of hydration per dimer.

The structures of these dimers are distinct from most other $A_2Cu_2X_6$ copper halide dimers whose structures have been determined, due to the coordination of the 3-aminopyridinium cation to the copper atom through the amino group. In previously studied copper halide oligomers with substituted aminopyridinium cations,[13–16] the aminopyridinium cations appeared as free cations, not coordinated to the copper atom. In these instances, the dimers aggregate to form infinite stacks with semicoordinate bonds between adjacent dimers. The direct amino coordination in the 3AP salts leads to the formation of isolated dimers, which results in five-coordinate copper(II) with a distorted-trigonal-bipyramidal geometry. Similar coordination behavior of a multidentate cation has been observed with the purinium,[17] adeninium,[18] and guaninium[19] cations.

The distortion from trigonal-bipyramidal geometry in the chloride complex is most obvious in bond angles in the equatorial plane, which range from 102.2 to 146.6°, showing considerable

(12) *International Tables for X-ray Crystallography*; Kynoch: Birmingham, England, 1974; Vol. IV.

(13) Grigereit, T. E.; Ramakrishna, B. L.; Place, H.; Willett, R. D.; Pellacani, G. C.; Manfredini, T.; Menabue, L.; Bonamartini-Corradi, A.; Battaglia, L. P. *Inorg. Chem.* **1987**, *26*, 2235.

(14) Geiser, U.; Gaura, R. M.; Willett, R. D.; West, D. X. *Inorg. Chem.* **1986**, *25*, 4203.

(15) Halvorson, K. E.; Grigereit, T.; Willett, R. D. *Inorg. Chem.* **1987**, *26*, 1716.

(16) Place, H.; Willett, R. D. *Acta Crystallogr., Sect. C: Cryst. Struct. Commun.* **1987**, *C43*, 1050.

(17) Sheldrick, W. S. *Acta Crystallogr., Sect. B: Struct. Crystallogr. Cryst. Chem.* **1981**, *B37*, 945.

(18) Brown, D. B.; Hall, J. W.; Helis, J. M.; Walton, E. G.; Hodgson, D. J.; Hatfield, W. E. *Inorg. Chem.* **1977**, *16*, 2675.

(19) Carrabine, J. A.; Sundaralingam, M. *J. Am. Chem. Soc.* **1970**, *92*, 369.

deviation from ideal 120° angles. The bond opposed to this large angle (Cu–Cl(3)) is somewhat elongated at 2.496 (1) Å, as compared to 2.320 (1) and 2.279 (1) Å for the other two bonds. The large angle, Cl(1)-Cu-Cl(2a), is typical of the folded 4 + 1 geometry frequently assumed by copper(II) halides. However, the Cu–Cl (3) bond is considerably shorter than normally found in that typical geometry.[20] The coordination geometry is closer to trigonal bipyramidal than for any other halide salt with the exception of the guaninium salt[19] and the $Cu_4Cl_6OL_4$ clusters where, in the latter, it is constrained to that geometry.[21] To distinguish between coordinate and semicoordinate bonds, the criteria that we have frequently used is whether the chlorine–chlorine contacts are shorter or longer than the sum of the ionic radii (3.6 Å). In this compound, the contacts between Cl(3) and the two "axial" ligands, Cl(2) and N(1), are near or less than this value. Thus, the classification as trigonal bipyramidal has some justification despite the angular distortion in the equatorial plane.

The dimer structure itself is quite similar to that of other symmetrically bibridged copper chloride dimers.[22] The bridging distances are slightly longer than 2.3 Å while the nonelongated, nonbridging distance (Cu–Cl (1)) is somewhat less than 2.3 Å. The bridging Cu–Cl–Cu angle is 94.9 (1)°. For magnetic reasons, it is interesting to compare the geometric structure observed in Figure 1 with those of a series of $Cu_2Cl_6^{2-}$ dimers that have been studied.[20,25] These have been characterized by a bifolded (or "sedia") geometry with a bifold angle, σ, between the central Cu_2Cl_2 plane and, in this case, the plane defined by Cu, N(1), Cl(1) and Cl(2) (see Figure 1). For this 3AP dimer, σ is 32.5°, which corresponds to one of the larger bifold angles observed. Contacts between adjacent dimers in the structure (other than contacts involving the pyridinium ring) are minimal, with no Cl···Cl interaction less than 3.87 Å. Thus, the system can be expected to behave magnetically as an array of nearly isolated dimers.

The bromide dimer, $(3AP)_2Cu_2Br_6 \cdot H_2O$ (Figure 2), again shows the unique coordination of the aminopyridinium amino group to the copper atom, resulting in five-coordinate copper(II). In this case, though, there are clearly four normal coordinate bonds and one longer "semicoordinate" bond, Cu–Br(1a), of 2.791 (2) Å to one of the bridging bromide ions. Intradimer contacts of Br(1a) with Br(2), Br(3), and N(2) are 4.249, 4.288, and 3.432 Å, respectively, substantially larger than the sum of the ionic radii (3.9 Å, Br–Br; 3.4 Å, Br–N), so this bond is truly of the semicoordinate variety. (The Br(1) contact with Br(1a) within the bridge is only 3.605 Å, but this is to be expected.) Surprisingly, the angular distortion of the equatorial plane is less than in the chloride salt with angles ranging from 109.3 to 139.9°.

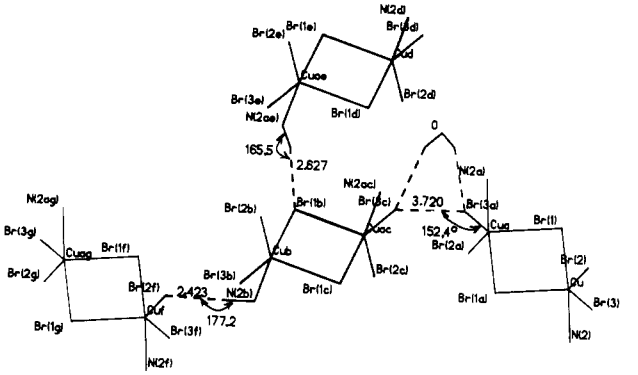

Figure 3. Illustration of possible interdimer magnetic exchange pathways in $(3AP)_2Cu_2Br_6 \cdot H_2O$. The short Br–Br and N–H···Br contacts between dimers are shown.

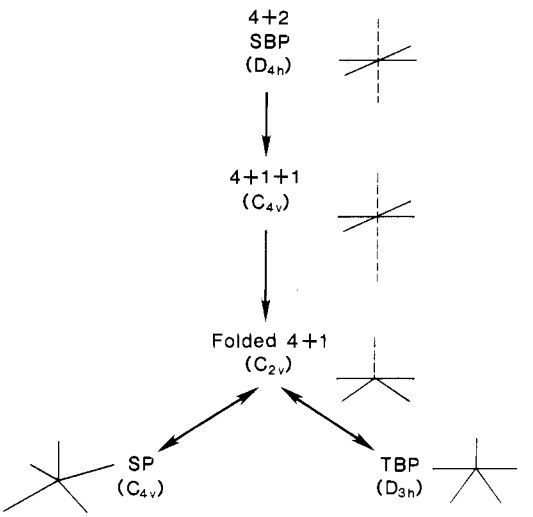

Figure 4. Distortion pathways for five- and six-coordinate copper(II) halide species.

In a comparison of the chloride and bromide dimers in Figures 1 and 2, it is seen that the elongated bond has a different orientation within the two dimers. For the bromide salt, the semicoordinate Cu–Br bond is involved in the bridge formation, forming an asymmetric bibridged arrangement, with a bridging Cu–Br–Cu angle of 93.4°. This bridging arrangement is similar to that seen in a variety of copper(II) halide dimers. Again, for the normal coordinate bonds, the bridging Cu–Br(1) distance (2.451 (2) Å) is significantly longer than the terminal Cu–Br(2) and Cu–Br(3) bonds (2.413 (2) and 2.412 (2) Å, respectively).

An important feature of the bromide structure is the role of the water of hydration. In the crystal lattice, two symmetry-related pyridinium ions form hydrogen bonds to each oxygen atom while the OH groups hydrogen bond in turn to symmetry-related Br(3) ions on adjacent dimers. This holds these bromide ions 3.728 Å apart, which is much less than the sum of the bromide ion van der Waals radii (Figure 3). The Cu–Br···Br angle is 152.4°. As a result, these bromide ions on adjacent dimers interact strongly; the magnetic implications of this interaction will be discussed below. Other short interdimer interactions are also noted in Figure 3.

Structural Correlations. The geometries of five-coordinate copper complexes are quite varied (see Figure 4). The idealized symmetrical end members of square-pyramidal (SP) and trigo-

(20) Willett, R. D. *Transition Met. Chem. (Weinheim, Ger.)*, in press.
(21) Bertrand, J. A.; Kelley, J. A. *Inorg. Chem.* **1969**, *8*, 1982. Bertrand, J. A. *Inorg. Chem.* **1967**, *6*, 495. Dickson, R. C.; Helun, F. T.; Baker, W. A.; Black, T. D.; Watson, W. H. *Inorg. Chem.* **1977**, *16*, 1530.
(22) Geiser, U.; Willett, R. D.; Lindbeck, M.; Emerson, K. *J. Am. Chem. Soc.* **1986**, *108*, 1173.
(23) Muetterties, E. L.; Guggenberger, L. J. *J. Am. Chem. Soc.* **1974**, *96*, 1748.
(24) (a) Marsh, W. E.; Patel, K. C.; Hatfield, W. E.; Hodgson, D. J. *Inorg. Chem.* **1983**, *22*, 511. (b) Hodgson, D. J.; Hale, P. K.; Hatfield, W. E. *Inorg. Chem.* **1971**, *10*, 1065. (c) Duckworth, V. F.; Stephenson, N. C. *Acta Crystallogr., Sect. B: Struct. Crystallogr. Cryst. Chem.* **1969**, *B25*, 1795. (d) Swank, D. D.; Needham, G. F.; Willett, R. D. *Inorg. Chem.* **1979**, *18*, 761. (e) Marsh, W. E.; Hatfield, W. E.; Hodgson, D. J. *Inorg. Chem.* **1982**, *21*, 2679. (f) Hoffmann, S. K.; Hodgson, D. J.; Hatfield, W. E. *Inorg. Chem.* **1985**, *24*, 1184. (g) Marsh, W. E.; Eggleston, D. S.; Hatfield, W. E.; Hodgson, D. J. *Inorg. Chim. Acta* **1983**, *70*, 137. (h) Braithwaite, A. C.; Richard, C. E. F.; Waters, T. N. *J. Chem. Soc.* **1975**, 1817. (i) Phelps, D. W.; Goodman, W. H.; Hodgson, D. J. *Inorg. Chem.* **1976**, *15*, 2266. (j) Knapp, S.; Toby, B. H.; Sebastian, M.; Krogh-Jespersen, K.; Potenza, J. A. *J. Org. Chem.* **1981**, *46*, 2490. (k) Svedung, D. H. *Acta Chem. Scand.* **1969**, *23*, 2865. (l) Beckingsak, P. G.; Morcom, A. T.; Rickard, C. E. F.; Waters, T. N. *J. Chem. Soc., Dalton Trans.* **1977**, 2135.
(25) (a) Willett, R. D. *J. Chem. Phys.* **1966**, *44*, 39. (b) Willett, R. D. *Transition Met. Chem. (Weinheim, Ger.)*, in press. (c) Roberts, S. A.; Bloomquist, D. R.; Willett, R. D.; Dodgen, H. W. *J. Am. Chem. Soc.* **1981**, *103*, 2603. (d) Battaglia, L. P.; Bonamartini-Corradi, A.; Geiser, U.; Willett, R. D.; Motori, A.; Sandrolini, F.; Antolini, L.; Manfredini, T.; Menabue, L.; Pellacani, G. C. *J. Chem. Soc., Dalton Trans.*, in press. (e) Scott, B. S.; Willett, R. D. *Inorg. Chim. Acta* **1987**, *141*, 193. (f) Battaglia, L. P.; Bonamartini-Corradi, A.; Marcotrigiano, G.; Menabue, L.; Pellacani, G. C. *Inorg. Chem.* **1980**, *19*, 125. (g) Harlow, R. L.; Wells, W. J.; Watt, G. W.; Simonsen, S. H. *Inorg. Chem.* **1974**, *13*, 2860. (h) Murray-Rust, P. *Acta Crystallogr. Sect. B: Struct. Crystallogr. Cryst. Chem.* **1975**, *B31*, 1771. (i) Colombo, A.; Menabue, L.; Motori, A.; Pellacani, G. C.; Porzio, W.; Sandrolini, F.; Willett, R. D. *Inorg. Chem.* **1985**, *24*, 2900. (j) Sheldrick, W. S. *Acta Crystallogr. Sect. B: Struct. Crystallogr. Cryst. Chem.* **1981**, *B37*, 945. (k) Bukawska-Strayzewska, M.; Tosik, A.; Glowiak, T.; Wnek, J. *Acta Crystallogr., Sect. C: Cryst. Struct. Commun.* **1985**, *C41*, 1184.

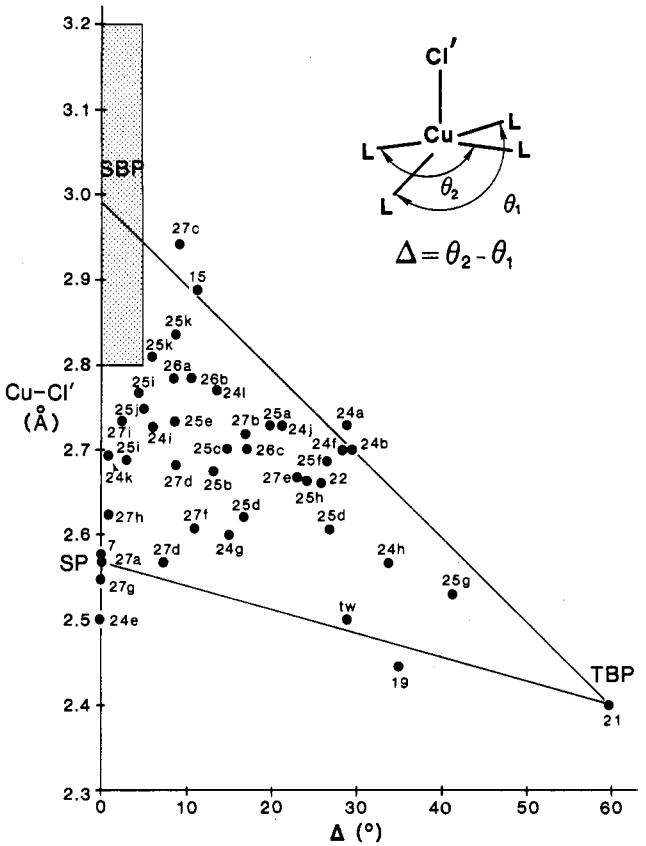

Figure 5. Plot of semicoordinate Cu–Cl distance versus the angular distortion, Δ, for five-coordinate copper(II) chloride species. The numbers refer to references in this paper; the symbol "tw" denotes "this work".

nal-bipyramidal (TBP) geometries are observed rather rarely. Instead a rather ill-defined stereochemistry involving four normal copper–ligand (Cu–L) bonds and one longer, so-called semicoordinate (Cu–L′) bond is commonly observed. This is usually refered to as a 4 + 1 geometry. The four normal bonds often approximate an arrangement close to square planar, and it is convenient to describe the geometry by two so-called "trans" L–Cu–L angles, θ (Figure 5). Thus, if the species tends toward SP, $\theta_1 \sim \theta_2$, while in the TPB limit $\theta_1 \rightarrow 120°$ and $\theta_2 \rightarrow 180°$. Thus, three parameters, the Cu–L′ distance, θ_1, and θ_2, serve to give a rough description of the stereochemistry of the 4 + 1 species. However, to more completely describe the geometry, it is necessary to specify the L–Cu–L′ angles since a significant number of 4 + 1 species distort toward tetrahedral geometry ($\theta_1 < 180°$, $\theta_2 > 180°$) for the CuL_4 moiety. In the subset of the 4 + 1 geometries that excludes the tetrahedral distortion, a large number have an elongated Cu–L′ distance with $\theta_2 \sim 180°$. (We have not been rigorous in excluding all distorted tetrahedral geometries for which θ_2 is only slightly larger than 180°.) We will refer to this as a folded geometry. A more precise description of the geometry can be obtained by application of Muetterties and Guggenberger's prescription involving dihedral angles between the various faces of the CuL_4L' polyhedra.[23] However, these are rarely tabulated in the literature and can only be applied when all of the L and L′ ligands have the same radii.

A large number of structures of copper(II) halide salts have now been determined, particularly when the halide is the chloride ion. It is of interest to examine the stereochemistries of the five-coordinate species so studied and to search for trends. In particular, it is of interest to see if it is possible to define a pathway for the transformation from the SP to the TBP geometry. A potential surface can be envisioned for this transformation. In the absence of perturbation due to the lattice, all species should conform to the geometry defined by the minimum in this surface. However, interactions with the surroundings will perturb this surface, yielding the observed variations in geometries. Nevertheless, the results should tend to cluster in the low-energy regions of the surface. Thus, as more structures are determined, it should be possible to obtain an increasingly accurate view of the surface.

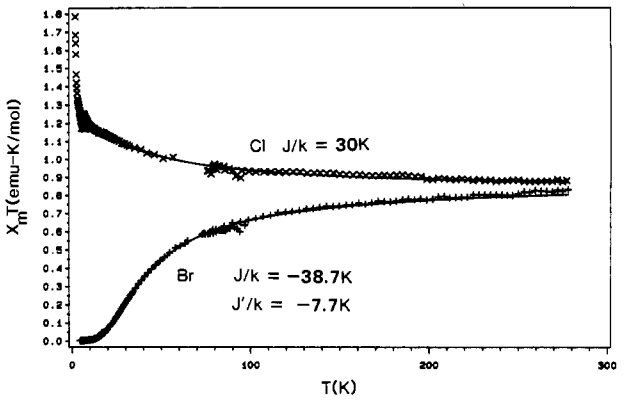

Figure 6. Plot of $\chi_M T$ versus T for $(3AP)_2Cu_2Cl_6$ (upper) and $(3AP)_2Cu_2Br_6 \cdot H_2O$ (lower). The solid curves are computed from the models and parameters described in the text.

To describe the SP to TBP surface, the structural data on a large number of folded copper(II) chloride salts and/or complexes have been tabulated with the requirement that L′ and at least two of the L ligands are chloride ions. This includes a series of asymmetrically bibridged dimers,[24] stacks of bifolded dimers,[25] monobridged chains,[26] and miscellaneous monomeric and oligomeric salts.[13,15,27] In order to present the data in an easily visuallized manner, Figure 5 plots the Cu–L′ distance versus $\Delta = \theta_2 - \theta_1$, the difference between the two trans angles. This two-dimensional plot is not unambiguous, since it does not indicate the deviations of the θ_2 values from 180°. However, θ_2 is normally in the range 170–180°, except for the square-pyramid limit. The points labeled SP and TBP define the square-pyramidal (in $(C_6H_{18}N_3)CuCl_5 \cdot 2H_2O$[27a]) and trigonal-bipyramidal (in the $Cu_4Cl_6OL_4$ clusters[21]) limits. Also indicated by the shaded region is the square-bipyramidal limit, designated by SBP, of the 4 + 2 coordination geometry. In this geometry, found in a large number of $(RNH_3)_2CuCl_4$,[28] $CuCl_2L_2$,[29] and some planar $Cu_2Cl_6^{2-}$ dimer systems,[30] the semicoordinate bonds typically range from 2.8 to 3.2 Å. As can be seen, there is a wide scatter of geometries represented on this diagram. Nevertheless, it is possible to observe a preferred region on this section of the potential surface defined by a Cu–Cl′ distance in the range 2.65–2.75 Å and 15° < Δ < 30°. This folded 4 + 1 stereochemistry then must be recognized

(26) (a) Copeland, V. C.; Hatfield, W. E.; Hodgson, D. J. *Inorg. Chem.* **1973**, *12*, 1340. (b) Bream, R. A.; Estes, E. D.; Hodgson, D. J. *Inorg. Chem.* **1975**, *14*, 1672. (c) Willett, R. D.; Chang, K. *Inorg. Chim. Acta* **1970**, *4*, 447.

(27) (a) Antolini, L.; Marcotrigiano, G.; Menabue, L.; Pellacani, G. C. *J. Am. Chem. Soc.* **1980**, *102*, 1303. (b) Antolini, L.; Marcotrigiano, G.; Menabue, L.; Pellacani, G. C. *J. Am. Chem. Soc.* **1980**, *102*, 5506. (c) Caputo, R. E.; Vukosavovich, M. J.; Willett, R. D.; *Acta Crystallogr., Sect. B: Struct. Crystallogr. Cryst. Chem.* **1976**, *B32*, 2516. (d) Haije, W. G.; Dobbelaar, J. A. L.; Maaskant, W. J. A. *Acta Crystallogr., Sect. C: Cryst. Struct. Commun.* **1986**, *C42*, 1485. (e) Willett, R. D.; Geiser, U. *Inorg. Chem.* **1986**, *25*, 4558. (f) Marsh, W. E.; Hatfield, W. E.; Hodgson, D. J. *Inorg. Chem.* **1983**, *22*, 2899. (g) Geiser, U.; Gaura, R. M.; Willett, R. D.; West, D. X. *Inorg. Chem.* **1986**, *25*, 203. (h) De Munno, G.; Denti, G.; Dapporto, P. *Inorg. Chim. Acta* **1983**, *74*, 199. (i) Sletton, E.; Apeland, A. *Acta Crystallogr., Sect. B: Struct. Crystallogr. Cryst. Chem.* **1975**, *B31*, 2019.

(28) Smith, D. W. *Coord. Chem. Rev.* **1976**, *21*, 93.

(29) (a) Harker, D. *Z. Kristallogr. Kristallgeom., Kristallphys., Kristallchem.* **1936**, *93*, 136. (b) Morosin, B. *Acta Crystallogr., Sect. B: Struct. Crystallogr. Cryst. Chem.* **1975**, *B31*, 632. (c) Marsh, W. E.; Valente, E. J.; Hodgson, D. J. *Inorg. Chim. Acta* **1981**, *51*, 49. (d) Endres, H. *Acta Crystallogr., Sect. C: Cryst. Struct. Commun.* **1983**, *C39*, 1192. (e) Mignamisi-Bélombé, M.; Singh, P.; Bolster, D. E.; Hatfield, W. E. *Inorg. Chem.* **1984**, *23*, 2576.

(30) (a) Willett, R. D.; Dwiggens, C.; Kruh, R. F.; Rundle, R. E. *J. Chem. Phys.* **1963**, *39*, 54. (b) Willett, R. D.; Rundle, R. E. *J. Chem. Phys.* **1964**, *40*, 838. (c) Vossos, P. H.; Fitzwater, D. R.; Rundle, R. E. *Acta Crystallogr.* **1963**, *16*, 1037. (d) Swank, D. D.; Willett, R. D. *Inorg. Chem. Acta* **1974**, *8*, 143. (e) Manfredini, T. Ph.D. Thesis, University of Modena and Bologna, Italy, 1984.

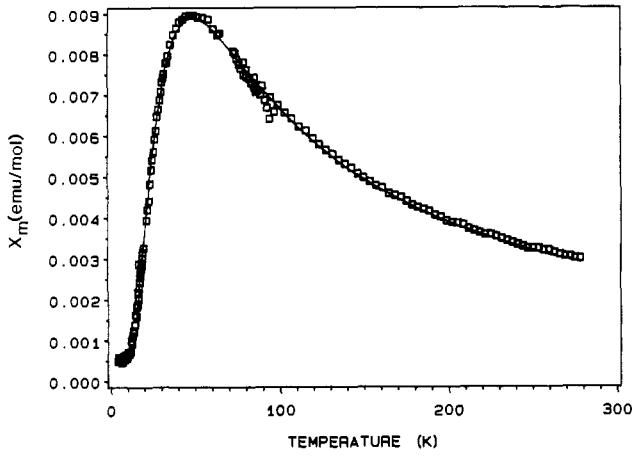

Figure 7. Plot of χ_M versus T for $(3AP)_2Cu_2Br_6 \cdot H_2O$. The solid curve is computed from the model and parameters described in the text.

as the dominant five-coordinate geometry in copper(II) halide chemistry. Conspicuous in their absence, other than in the $Cu_4Cl_6OL_4$ clusters, are geometries approaching the TBP limit. Thus the experimental evidence demonstrates that this geometry is not favored, as argued theoretically by Reinen.[31] There are a number of compounds in which the geometries approach the SP limit, which indicates that the potential surface has a rather low energy in this limit. An interesting question, unresolved by the data at this point, is whether or not a potential barrier exists between the SP and folded 4 + 1 geometries. Finally, it is noted that only two compounds exist along the direct SP ↔ TBP pathway, the 3-aminopyridinium salt described here and the similar guaninium dimer.[19] It can thus be concluded that a transformation of the $CuCl_5^{3-}$ ion from the square-pyramidal to the trigonal-bipyramidal conformation would occur via the folded 4 + 1 species.

Magnetic Behavior. From the plot of the product $\chi_m T$ vs T for $(3AP)_2Cu_2Cl_6$, shown in Figure 6, the magnetic interactions are clearly ferromagnetic. The data were fit to the Bleaney–Bowers dimer model with mean field correction (θ), resulting in ferromagnetic interactions with J/k = 30 (4) K and θ = 0.42 (1) with g = 2.12, the value obtained from the high-temperature Curie–Weiss plot. Because of the strong correlations of J with g, the uncertainties on J are quite large, and it should be concluded only that J has a large, positive value.

In contrast, the magnetic data for the bromide dimer (Figures 6 and 7) show antiferromagnetic coupling. An attempt to fit the data to the isolated dimer (Bleaney–Bowers) model gave a poor fit in the region of the maximum in χ. This suggested that interdimer coupling was important. Thus an alternating chain model, defined by

$$\mathcal{H} = -2J\sum_i (\vec{S}_{2i} \cdot \vec{S}_{2i+1} + \alpha \vec{S}_{2i+1} \cdot \vec{S}_{2i+2})$$

was used with $J' = \alpha J$ where α is the alternation parameter. When α is zero, the interaction is that of an isolated dimer; when α is one, the interaction is that of a linear chain. Using this model, the value of J was found to be −38.7 (1) K and α was found to be 0.20 (1) (J' = −7.7 (4) K).

Magnetostructural Correlations. In interpreting magnetic data in terms of magnetostructural correlations, the exchange coupling between metal centers is recognized to have contributions arising from two components, one ferromagnetic (J_F) and one antiferromagnetic (J_{AF}) with

$$J = J_F + J_{AF} \quad (1)$$

In the Hoffmann formalism,[32] the ferromagnetic contribution to the exchange is given by the coulomb integral, K_{AB}, and the antiferromagnetic contribution to the exchange is proportional to the square of the difference in energies between the two highest molecular orbitals derived from the local magnetic orbitals:

$$J_{AF} \propto (\epsilon_1 - \epsilon_2)^2 \quad (2)$$

For a copper(II) dimer, the complete exchange integral is given by

$$E_s - E_t = 2J = 2K_{ab} - (\epsilon_1 - \epsilon_2)^2/(J_{aa} - J_{ab}) \quad (3)$$

where E_s and E_t are the energies of the singlet and triplet states, respectively, and a and b are the localized magnetic orbitals centered on the two different metal atoms. Since K_{ab} is inherently positive and $J_{aa} > J_{ab}$, the sign of J is determined by the energy differences of the two highest molecular orbitals, $(\epsilon_1 - \epsilon_2)$. If these two orbitals are relatively close in energy, the magnetic coupling will be ferromagnetic, while a greater split in energies will induce an antiferromagnetic coupling. Calculations[32,33] have shown that $|\epsilon_1 - \epsilon_2|$ increases as the bridging Cu–X–Cu angle, ϕ, increases from 90°. These calculations have been confirmed by experimental observation of increasing antiferromagnetic character as ϕ is increased in a series of hydroxy[34] and alkoxy-bridged[35] systems. Experimentally, the factors that influence the magnetic coupling include both the Cu–X–Cu bridging angle, ϕ, and the coordination geometry. In particular, a good correlation has been found in $A_2Cu_2X_6$ salts between J and either the twist angle, τ,[36] or the bifold angle, σ.[37]

Extended Hückel calculations have been used to evaluate $(\epsilon_1 - \epsilon_2)$ for the bifolded chloride dimers.[5,37] The results of these calculations are in excellent agreement with experimental results, which have shown that, with $\phi \sim$ 95–96°, an increasingly ferromagnetic exchange interaction is observed as the bifold angle σ increases to 32°, with a crossover from antiferromagnetic to ferromagnetic coupling at ~25°. With ϕ = 94.9° and σ = 32.5° for the chloride dimer, in this study, the existence of a strong ferromagnetic coupling is consistent with these results. It has also been noted that substitution of pyridine for a halide ion in the coordination sphere tends to decrease the antiferromagnetic contribution to the exchange.[30d] Thus, this study of the chloride dimer reaffirms the magnetostructural correlation previously deduced for symmetrically bibridged copper halide systems.

Unlike other copper bromide dimers we have studied,[18] the structure of $(3AP)_2Cu_2Br_6 \cdot H_2O$ at first did not seem to correlate with the observed magnetic behavior. Although the bromide analogue of a copper chloride dimer is usually the more antiferromagnetic of the two,[38] the large difference in magnetic coupling was suspicious. In addition, neither the asymmetric Cu–Br–Cu bridging behavior nor the angular distortion revealed an explanation for the magnetic behavior, as can be seen by comparison with the data on related compounds.[36] In these systems, the value of $|J/k|$ is almost always less than 5 K. With the observation of the short interdimer contacts, attention was focused on intermolecular exchange pathways in an attempt to explain the observed magnetic behavior.

The existence of a very short interdimer Br···Br contact was mentioned previously. As illustrated in Figure 3, short amino N–H···Br contacts also exist as well as several longer (> 4.1 Å) Br···Br contacts between dimers (listed in Table Vc). It is likely these pathways account for the observed magnetic behavior. In $(NH_3C_2H_4NH_3)CuBr_4$, a short Br···Br contact of ~3.8 Å has led to an antiferromagnetic coupling of −68 K.[39] The 3.728-Å Br···Br contact can thus be unambiguously identified as the major exchange pathway in this system. Thus, the magnetic dimer consists

(31) Reinen, D.; Friebel, C. *Inorg. Chem.* **1984**, *23*, 791.
(32) Hay, P. J.; Thibeault, J. C.; Hoffmann, R. *J. Am. Chem. Soc.* **1975**, *97*, 4884.
(33) Bencini, A.; Gatteschi, D. *Inorg. Chim. Acta* **1978**, *31*, 11.
(34) Hatfield, W. E. In ref 1; p 555.
(35) Laurent, J. P.; Bonnet, J. J.; Nepreu, F.; Astheimer, H.; Walz, L.; Haase, W. *J. Chem. Soc., Dalton Trans.* **1982**, 2433; Mikuriya, M.; Okawa, H.; Kida, S. *Bull. Chem. Soc. Jpn.* **1982**, *55*, 1086.
(36) Willett, R. D. In ref 1; p 389.
(37) O'Brien, S.; Gaura, R. M.; Landee, C. P.; Ramakrishna, B. L.; Willett, R. D. *Inorg. Chim. Acta* **1987**, *141*, 83.
(38) Scott, B.; Willett, R. D. *J. Appl. Phys.* **1987**, *61*, 3289.
(39) Rubenacker, G. V.; Haines, D. N.; Drumheller, J. E.; Emerson, K. *J. Magn. Magn. Mater.* **1984**, *43*, 238. Halvorson, K.; Willett, R. D., submitted for publication in *Acta Crystallogr.*

of copper atoms from adjacent structural dimers. Since N–H···X interactions normally lead to ferromagnetic exchange, the J' coupling is likely due to intradimer coupling or to the longer interdimer Br···Br contacts.

Acknowledgment. We acknowledge the support of NSF Grants DMR-8219430 and INT-8219425. In addition, the X-ray diffraction facility was established through funds supplied by NSF Grant CHE-8408407 and by The Boeing Co.

Note Added in Proof. As noted in the paper, the local coordination geometries in $(3AP)_2Cu_2Cl_6$ and $(guaninium)_2Cu_2Cl_6$[19,40] are very similar. Indeed, the gross molecular geometries are nearly identical. Yet the 3AP salt is ferromagnetic ($J/k \approx 30$ K) while the latter is strongly antiferromagnetic ($J/k = -59$ K).[41] It is worthwhile to determine whether there is a structural explanation and, indeed, if an intradimer source for the difference exists (in contrast to the new interdimer interaction in $(3AP)_2Cu_2Br_6 \cdot H_2O$). In reference to Figure 1, the pertinent distances and angles in the 3AP and guaninium salts are as follows: Cu–Cl(3), 2.496 vs 2.365 Å; Cl(2)–Cu–Cl(1a), 146.6 vs 134°; Cu–Cl(2), 2.320 vs 2.288 Å; Cu–Cl(2a), 2.330 vs 2.447 Å; Cu–Cl(2)–Cu, 97.9 vs 98°. While many features are similar, two important differences exist. The longer Cu–Cl bond has switched orientation, and thus the orientation of the magnetic orbitals will have changed. However, this factor may not be too significant since, for these geometries, the unpaired electrons will be in a strongly mixed combination of $d_{x^2-y^2}$ and d_{z^2} orbitals. Thus, the unpaired electron density at the bridging sites probably does not vary much for the two orientations. The more significant difference in this case would appear to be the bridging Cu–Cl–Cu angles, which are 3.1° larger for the guaninium complex than for the 3AP complex. A decrease in the value of J/k by 25–30 K per degree of angular variation is not unreasonable. Thus, this effect is clearly capable of accounting for the bulk of the observed variations in J.

Registry No. $[(C_5H_5N)NH_2]_2Cu_2Cl_6$, 112196-26-6; $[(C_5H_5N)NH_2]_2Cu_2Br_6 \cdot H_2O$, 112196-27-7.

Supplementary Material Available: Tables of thermal parameters and derived hydrogen positions (3 pages); listings of calculated and observed structure factors for both compounds (31 pages). Ordering information is given on any current masthead page.

(40) Sundaralingam, M.; Carrabine, J. A. *J. Mol. Biol.* **1971**, *61*, 287. Declereq, J. P.; Debbaudt, M.; Van Meerssche, M. *Bull. Soc. Chim. Belg.* **1971**, *80*, 527.
(41) Drake, D. F.; Crawford, V. H.; Laney, N. W.; Hatfield, W. E. *Inorg. Chem.* **1974**, *13*, 1246. Villa, J. F. *Inorg. Chem.* **1973**, *12*, 2054.

Contribution from the Département de Chimie Minérale, Analytique et Appliquée, and the Laboratoire de Cristallographie, University of Geneva, 30 quai Ernest Ansermet, 1211 Genève 4, Switzerland

2,2′-Bis(6-(2,2′-bipyridyl))biphenyl (TET), a Sterically Constricted Tetradentate Ligand: Structures and Properties of Its Complexes with Copper(I) and Copper(II)

Edgar Müller,*† Claude Piguet,† Gérald Bernardinelli,‡ and Alan F. Williams†

Received May 5, 1987

The synthesis of a new sterically constrained tetradentate N_4 ligand, 2,2′-bis(6-(2,2′-bipyridyl))biphenyl ($C_{32}H_{22}N_4$ = TET (I)), is presented. Its Cu(I) and Cu(II) complexes have been prepared and characterized with the aid of crystal structure analyses, electrochemistry, and electronic spectroscopy. $[Cu^I(TET)]ClO_4 \cdot 2CH_3CN$ ($C_{32}H_{22}N_4Cu(ClO_4) \cdot 2C_2H_3N$) (II) crystallizes in the triclinic system ($P\bar{1}$) with a = 10.585 (2) Å, b = 13.580 (3) Å, c = 14.025 (2) Å, α = 61.18 (1)°, β = 84.67 (1)°, γ = 70.93 (1)°, and Z = 2. The pseudotetrahedral cation $[Cu^I(TET)]^+$ shows a quasi-reversible Cu^I/Cu^{II} oxidation–reduction wave in the cyclic voltammogram at +0.94 V (NHE) in the noncoordinating solvent CH_2Cl_2 (counterion ClO_4^-) and has a strong metal-to-ligand charge-transfer absorption at 465 nm (ϵ = 4400). In coordinating solvents (acetonitrile, tetramethylurea), the Cu^I/Cu^{II} potential drops, indicating coordinative changes upon oxidation. A stability constant log K of 6.9 (1) was determined for the reaction TET + $Cu^+ \rightleftharpoons [Cu(TET)]^+$ in acetonitrile. $[Cu^{II}(TET)Cl]ClO_4 \cdot CH_3CN$ ($C_{32}H_{22}N_4CuCl(ClO_4) \cdot C_2H_3N$) (III) crystallizes in the monoclinic system ($P2_1/c$) with a = 12.860 (2) Å, b = 17.036 (3) Å, c = 14.585 (2) Å, $\alpha = \gamma$ = 90°, β = 96.33 (2)°, and Z = 4. The cation $[Cu^{II}(TET)Cl]^+$ is five-coordinate, showing a distorted trigonal-bipyramidal arrangement of the donor atoms. Cl^- occupies an equatorial position.

Introduction

There is currently considerable interest in the synthesis of new ligands whose structure is such as to define quite precisely the stereochemistry of their complexation to a metal ion. In particular, in the chemistry of copper, which shows a variety of coordination geometries in both the +I and the +II oxidation state, the properties of the central ion are largely controlled via the imposed coordination environment. Diimine ligands, such as 2,2′-bipyridyl or 1,10-phenanthroline and substituted derivatives thereof, are known to enhance the stability of the Cu(I) oxidation state relative to Cu(II),[1] especially when tetrahedral coordination is favored by the presence of bulky substituents, as in the cases of the 2,9-disubstituted 1,10-phenanthrolines[2] or the 6,6′-disubstituted bipyridines,[3] or by use of *catenand* type ligands.[4] Another approach, recently reported for some Ni(II) compounds, is to vary the distance between two bidentate subunits within a N_4 macrocycle until strain effects in the bridges favor the adoption of a tetrahedral over the more usual planar structure. Lippard and co-workers[5] showed two aliphatic bridges of six CH_2 groups between two diimine subunits to be an optimal choice in order to achieve a tetrahedral environment. In the case of the corresponding Cu(II) complexes, however, the 6,6 system was too flexible, and only a dinuclear species could be obtained.[6]

Our new approach, the open-chain ligand 2,2′-bis(6-(2,2′-bipyridyl))biphenyl (TET (I)), is also based upon a bridge of six carbon atoms joining two diimine subunits. In order to limit flexibility, all atoms of the ligand are parts of aromatic six-membered rings. Through intramolecular rotations around the single bonds joining the aromatic rings, the ligand may readily provide a pseudotetrahedral coordination geometry, but in no case a square-planar one. The use of twisted biphenyl "spacers" has recently been reported for a CuN_2S_2 chromophore[7] and for a CuN_4

† Département de Chimie Minérale, Analytique et Appliquée.
‡ Laboratoire de Cristallographie.

(1) James, B. R.; Williams, R. J. P. *J. Chem. Soc.* **1961**, 2007.
(2) Dietrich-Buchecker, C. O.; Marnot, P. A.; Sauvage, J.-P.; Kirchhoff, J. R.; McMillin, D. R. *J. Chem. Soc., Chem. Commun.* **1983**, 513.
(3) (a) Burke, P. J.; McMillin, D. R.; Robinson, W. R. *Inorg. Chem.* **1980**, *19*, 1211. (b) Burke, P. J.; Henrick, K.; McMillin, D. R. *Inorg. Chem.* **1982**, *21*, 1881.
(4) Albrecht-Gary, A.-M.; Saad, Z.; Dietrich-Buchecker, C. O.; Sauvage, J.-P. *J. Am. Chem. Soc.* **1985**, *107*, 3205.
(5) Davis, W. M.; Roberts, M. M.; Zask, A.; Nakanishi, K.; Nozoe, T.; Lippard, S. J. *J. Am. Chem. Soc.* **1985**, *107*, 3864.
(6) (a) Davis, W. M.; Zask, A.; Nakanishi, K.; Lippard, S. J. *Inorg. Chem.* **1985**, *24*, 3737. (b) Davis, W. M.; Lippard, S. J. *Inorg. Chem.* **1985**, *24*, 3688.
(7) Anderson, O. P.; Becher, J.; Frydendahl, H.; Taylor, L. F.; Toftlund, H. *J. Chem. Soc., Chem. Commun.* **1986**, 699.

0020-1669/88/1327-0849$01.50/0 © 1988 American Chemical Society